The Effects of Carbon Black Dust on Cumulus-Scale Convection

CHING-SEN CHEN
University of Illinois, Urbana 61801

HAROLD D. ORVILLE
Institute of Atmospheric Sciences, South Dakota School of Mines and Technology, Rapid City 57701

(Manuscript received 25 March 1976, in revised form 7 March 1977)

ABSTRACT

The effect of seeding with carbon black dust in the tropical atmosphere is simulated in a two-dimensional time-dependent cloud model which covers a region 6.4 km $\times$3.2 km in the x and z directions with 200 m grid intervals. Initial conditions are taken from the mean "hurricane season" soundings for the West Indies area (Jordan, 1958). An equation for the continuity of carbon black dust is added to the model. Scavenging of the carbon black dust by precipitation and cloud water content and diffusion of carbon dust to the ocean surface are included in the model. Radiative heating of the atmosphere by the carbon black is simulated. The heating rate is set proportional to the concentration of carbon black dust at a grid point. Air motion is simulated by horizontal density differences caused by horizontal gradients of the heating rate. The circulations lead to cooling and moistening in updrafts and warming and drying in downdrafts in a conditionally stable atmosphere. In the meantime, the carbon black is redistributed.

Three cases are used to test the concept of carbon black dust seeding. The first is a case having a horizontally homogeneous concentration of carbon black, namely, an "Even" case. This case shows that the atmosphere is heated by carbon particles but that no air motion occurs. Changing the initial distribution of carbon black dust to a "rectangular" pattern with gradations of carbon black concentration results in a second case called the "Layer-A" case. In this case, the vertical velocity decreases very rapidly with time after it passes its maximum value of 27 cm s^{-1} at 10 min. Eighteen percent of the original carbon black dust is lost in 100 min due primarily to diffusion to the ocean surface. Changing the dew-point curve in the mean sounding and using the initial carbon black dust pattern of the layer-A case results in a "Layer-B" case, the third case. A small cloud forms in this case. Comparison of the total amount of carbon black in the Layer-A and Layer-B case shows that small amounts of cloud and rain are not an efficient mechanism to deplete the carbon particles; these water contents do, however, decrease the solar energy absorbed by carbon black particles and hence weaken air motion. The maximum value of the vertical velocity increases by 15 cm s^{-1} if solar insolation can pass through cloud and rain without any loss.

Results of this numerical study are not encouraging for the *direct* formation of cloud lines by the spread of carbon black dust in the tropical atmosphere, unless the atmosphere is much more humid than normal. No conclusions concerning mesoscale effects of the solar heating and *indirect* formation of cloud lines are possible within the framework of this cloud-scale model.

1. Introduction

Currently several methods are used for cloud modification. Among these are the use of an ice-phase seeding agent to increase precipitation embryos and/or to modify cloud dynamics by releasing latent heat of fusion in supercooled clouds, and water spray to increase precipitation embryos in warm clouds. In addition, hygroscopic substances are used to produce precipitation embryos both in warm and supercooled clouds. In the past the concept of cloud modification by altering the radiative properties of clouds and the atmosphere has been proposed. So far, carbon black dust has been the substance used because carbon black dust can absorb solar energy and transfer almost all of the absorbed energy to the surrounding air very rapidly.

Some theoretical and experimental work was done in the 1950's. In 1958, the Naval Research Laboratory (Van Straten *et al.*, 1958) seeded eight cumulus clouds with carbon black dust. All of the clouds dissipated to some extent. In five seeding runs in clear air, small clouds formed in all cases. The Geophysics Research Directorate (Downie, 1960) made 18 runs seeding small clouds and clear air in October 1958–April 1959. Clear air seeding produced no obvious results. In "dissipating cloud seeding" some clouds dissipated, some did not. Some major shortcomings in these early experiments were given by Gray *et al.* (1974). These failings were:

1) The existing knowledge of the radiative properties of carbon black dust was inadequate.

2) The amount of carbon used was much too small (1–3 kg).

3) Severe clumping problem caused less solar radiation absorbed.

4) Observation and instrumentation capabilities were insufficient.

5) Seeding was applied on only a cumulus scale and not on the mesoscale.

Gray *et al.* (1976) proposes to overcome most of the previous experimental shortcomings by expanding the field tests to utilize many thousands of pounds of carbon black dust by manufacturing carbon black dust directly on the delivery vehicle and by more careful study and monitoring of the heating and meteorological effects. Gray proposes that the effects of carbon dust would be greater on the mesoscale (100–300 km on a side and 1–2 days' time duration). Also he believes that the horizontal diffusion processes are negligible in the mesoscale situation (at least for half a solar heating day). In our current study, we test the carbon dust hypothesis on the cumulus scale; the results are *not* directly applicable to the Gray hypothesis. Horizontal and vertical diffusion processes both exist on this scale. Our purpose is to see how carbon black generates cloud-scale air motions and whether it might lead to cloud formation in a few hours of heating. We use a two-dimensional time-dependent numerical cloud model to test certain aspects of the theory. We do not emphasize cloud formation or dissipation at this time, although one case does consider the effects of cloud formation on carbon black. Certain results are applicable to the cloud-scale experiments of Van Straten *et al.* (1958), but the quantities of carbon black simulated in the numerical experiments are much greater than those in the past field experiments.

The current techniques superimposed on longer running mesoscale models interacting with cloud-scale models may give further insight into the cloud-scale carbon black interactions with the mesoscale and vice versa.

The basic formulation of the cloud model (exclusive of the lower boundary) is similar to the work of Orville *et al.* (1972). The main difference is the application of carbon black dust to initialize air motion instead of using random perturbations of temperature and water vapor in the lower boundary layer. Air motion is caused by the establishment of temperature gradients which are due to the horizontal gradients of carbon black concentration. Water vapor is pumped into the cloud model from the ocean surface which is 10 m below the lower boundary grid points of the cloud model.

Three different cases are presented in this study. A distribution of carbon black with a horizontally homogeneous concentration is first tested. We call this case an "Even" case. This case shows that the atmosphere is heated by carbon black but that no motion is generated, a scale effect of the model. A "rectangular" gradation of carbon black concentration is constructed for another case, the "Layer-A" case. This case shows that atmospheric circulations are generated by the horizontal gradients of carbon black. Finally, modifying the dew-point curve in the Layer-A case and using the initial distribution of carbon black of the Layer-A case, we obtain a "Layer-B" case, which produces a small cloud.

2. Carbon black dust

a. Some properties of carbon black dust

Some properties of carbon black dust have been presented by Gray *et al.* (1974). These are as follows:

- Carbon black dust consists of fine essentially spherical particles composed of 95–99% pure carbon, the remainder being made up of volatile materials.
- The density of carbon black dust ρ_{cb} is 2 g cm^{-3}.
- Carbon black dust is hydrophobic so that it does not absorb water vapor.
- Carbon black dust is inert and non-toxic (Gray *et al.*, 1976).
- Particles of 0.1 μm radius maximize the solar absorption per unit mass, but this size is not critical (Gray *et al.* 1976). In this study, we assume that all carbon black dust particles have the same size, i.e., radius $r_{cb}=0.1$ μm.
- The fallspeed of 0.1 μm particles is negligible ($\sim$20 cm day^{-1}).
- Carbon black dust has high radiation absorptivity and low heat capacity (0.125 cal g^{-1} °C^{-1}). Therefore, carbon black dust can heat the surrounding air primarily (about 94%) by direct energy absorption and rapid molecular conduction of this heat to the surrounding air. About 5% of the heat transfer from the carbon black dust to the air is accomplished by longwave radiation. Following Frank's study (1973), it is reasonable to assume that virtually all the radiation absorbed by carbon black dust will be directly converted into heat within the absorption layer.

b. Solar radiation energy absorbed by carbon black dust

Following Gray's calculation (1974), a table can be constructed from which one can understand the relationship between the energy absorbed by carbon black dust and its concentration. In Table 1, the area coverage is equal to the total cross section of carbon black dust, no overlap assumed, divided by the total horizontal seeding area; hence, for a given mixing ratio of carbon black dust, C_b(g g^{-1}), the percent area coverage may be written as

$$\frac{\rho C_b \Delta x \Delta y \Delta z 10^6}{\frac{4}{3}\pi r_{cb}{}^3 \rho_{cb}} \frac{\pi r_{cb}{}^2 10^2}{\Delta x \Delta y 10^4} = \frac{\rho C_b \Delta z 10^4}{\frac{4}{3} r_{cb} \rho_{cb}}, \quad (1)$$

where Δx and Δz are the grid intervals in x and z direc-

TABLE 1. Heating rates of carbon black dust and transmission of solar radiation energy.

Percent area coverage	Net heat absorbed in 10 h (cal cm^{-2})	Percent transmitted
0	0	100
5	60	92.5
9	110	86.25
18	200	75.00
26	270	66.25
35	325	59.375
53	410	48.75
70	470	41.25

tion, Δy is the unit length in y direction, and ρ (g cm^{-3}) is the density of air.

In the second column of Table 1, the net heat absorbed by carbon black dust is based on a 10% surface albedo.

In the third column of Table 1, the percent solar radiation transmitted is equal to the solar radiation at the bottom of an air layer divided by the incoming solar radiation at the top of the air layer times 100. The percent transmitted is less than 100 in Table 1 because of the absorption of solar radiation from carbon black dust. The effects of cloud water and raindrops on transmission are considered in the following section.

c. *Cloud albedo*

From Paltridge (1974), cloud albedo α is defined as $\alpha(\Delta x)=[R_{0s}\downarrow-R_s\downarrow(\Delta z)]/R_{0s}\downarrow$, where $R_{0s}\downarrow$ is the downward shortwave flux at the top of a cloud layer, $R_s\downarrow(\Delta z)$ is the downward flux at the bottom of a cloud layer and Δz is the depth of a cloud layer (Δz is 200 m in this study). This definition can be expressed by

$$\alpha(\Delta z)=(0.2\Delta z/L_p)/(1+0.2\Delta z/L_p), \qquad (2)$$

where L_p, the mean free path of light through clouds, is equal to

$$1/(\sum_i N_i\pi r_i^2),$$

and N_i is the number of cloud droplets or raindrops with radius r_i in a unit volume inside the cloud layer. We assume that the cloud droplets have uniform size in a cloud layer. Therefore, the mean radius r_c is 10 μm and N_i becomes $N_c=l_{cw}\rho/(\frac{4}{3}\pi r_c^3\rho_w)$, where l_{cw} is the mixing ratio of cloud droplets, and ρ_w the density of water. For raindrops

$$\sum_i N_i\pi r_i^2\int_0^\infty \pi\left(\frac{D_R}{2}\right)^2 N_{0R}\exp(-\lambda_R D_R)dD_R$$

from the Marshall-Palmer distribution, where D_R is the diameter of a raindrop, N_{0R} is a constant (0.08 cm^{-4}), $\lambda_R=(\pi\rho_w N_{0R}/\rho l_R)^{\frac{1}{4}}$, and l_R is the mixing ratio of rainwater.

When we treat the effect of cloud or rain on incoming solar radiation, we assume that (2) still holds as we divide the total cloud depth or rain region into many layers. We also assume that (2) is true for the effect on the incoming solar radiation. This assumption may not be good, but we think that the error will not be significant because rain begins to form only after l_{cw} is greater than 2 g kg^{-1}, and at this value the cloud albedo is about 0.875 from the effect of cloud water. That means only 15% of the incoming solar radiation will pass through this cloud layer so that the effect of rain on the transmission has no great significance.

From these assumptions for cloud water (2) becomes

$$\alpha_c(\Delta z)=\frac{0.2\Delta z l_{cw}\rho/(\frac{4}{3}r_c)}{1+0.2\Delta z l_{cw}\rho/(\frac{4}{3}r_c)},$$

and for rain

$$\alpha_R(\Delta z)=\frac{0.2\Delta z\pi N_{0R}/(\lambda_R{}^3 2)}{1+0.2\Delta z\pi N_{0R}/(\lambda_R{}^3 2)}.$$

Here $[1-\alpha_c(\Delta z)][1-\alpha_R(\Delta z)]$ is the transmitted portion of solar radiation passing through an air layer containing cloud water and rain.

3. Cloud model

a. *Assumptions and limitations*

1) The model is 6.4 km in width and 3.2 km in height with a grid interval of 200 m in the x and z directions. Every quantity is symmetrical about the z axis except the streamfunction and vorticity. These two quantities are asymmetric about the central axis.

2) A locally compressible fluid is assumed in the model atmosphere. The local rate of change of the initial density is assumed zero.

3) Eddy coefficients of momentum, heat and carbon black are the same in the beginning. Eddy coefficients depend on vorticity, deformation and Richardson number (Drake *et al.*, 1974).

4) Water vapor in excess of that required to saturate the air will condense to cloud water immediately. Similarly, a deficit below saturation in cloud air is immediately supplied by the evaporation of the cloud water.

5) The Marshall-Palmer distribution for raindrops is assumed. Raindrops are assumed to fall at their terminal velocity relative to the ambient wind.

6) The process of cloud water conversion to rainwater is parameterized.

7) The freezing process and Coriolis force are neglected.

b. *The hydrodynamic equations and cloud physics equations*

The hydrodynamic equations and cloud physics equations are the same as those of Liu and Orville (1969)

and Orville *et al.* (1972) except that there are no freezing processes in this current paper.

c. The continuity equation for carbon black dust

The continuity equation for carbon black dust is

$$\frac{\partial C_b}{\partial t} = -\mathbf{V}\cdot\nabla C_b + \frac{1}{\rho}\nabla\cdot K_h\nabla\rho C_b + \text{source} + \text{sink}. \quad (3)$$

The left-hand side of (3) is the local change of carbon black mixing ratio. On the right-hand side of (3), the first term is the advection term, with $\mathbf{V}$ the two-dimensional wind with components u (horizontal) and w (vertical); the second is the turbulence term; the third is a source term of carbon black dust; and the last is the sink of carbon black dust. The source and sink terms are developed below.

In this study, we assume that there is a distribution of carbon black dust inside the cloud model domain in the beginning and no additional sources as time goes on. There are two ways to reduce the total amount of carbon black dust via the sink term. The first is by diffusion at the lower boundary (a loss to the ocean surface). The second is collection by cloud water and raindrops. Carbon black dust particles collected by the cloud water and raindrops are assumed to be lost forever, even though the cloud water and raindrops may evaporate again. Quite likely, aggregation of the particles would occur within the drops. The total surface area of the aggregate particles would be considerably less than the sum of the surface area of the individual particles which are collected by cloud droplets or raindrops. Therefore, we neglect the heating effect due to these aggregate carbon particles.

1) SINK DUE TO DIFFUSION TERM

The analytical form for the diffusion term in the z direction at the lower boundary is

$$\frac{1}{\rho}\frac{\partial K_h}{\partial z}\frac{\partial(\rho C_b)}{\partial z} + \frac{1}{\rho}K_h\frac{\partial^2(\rho C_b)}{\partial z^2}.$$

The sink term for carbon black dust from diffusion is

$$\left[\frac{1}{\rho}K_h\frac{\partial^2(\rho C_b)}{\partial z^2}\right]_0 = \frac{2}{(\Delta z)^2}\left(\frac{K_h}{\rho}\right)_0 \times\left[\left(\frac{\rho C_b}{1+\theta_c}\right)_1 + \left(\frac{\rho C_b}{\theta_c^2+\theta_c}\right)_{-1} - \left(\frac{\rho C_b}{\theta_c}\right)_0\right], \quad (4)$$

where K_h is the eddy coefficient. The symbol 0 denotes the lower boundary of the cloud model, 1 denotes one layer above the lower boundary, -1 represents the surface of the ocean which is 10 m below the lower boundary points, and θ_c is the ratio 10 m/200 m. In (4), we assume that the concentration of carbon black dust at the ocean surface is always zero. Quite possibly this method leads to too rapid loss to the sea surface, but this is a first attempt. The loss does not have an important influence on the results.

2) SINK DUE TO CLOUD WATER

We assume the radius of all cloud droplets is 10 μm.

(i) Diffusion effect from Fuchs (1964). Carbon black diffuses onto the surface of cloud droplets; this sink term can be expressed by

$$\frac{\Delta C_b}{\Delta t} = -4\pi D_b C_b N_c r_c, \quad (5)$$

where D_b is 2.21×10^{-6} cm^2 s^{-1} for particles with radius 0.1 μm.

(ii) Sweep-out effect. Cloud droplets collect carbon particles. From Byers (1965), this term can be expressed by

$$\frac{\Delta C_b}{\Delta t} = -\pi r_c^2 C_b V_c E_c N_c, \quad (6)$$

where V_c, the terminal velocity of cloud water, is equal to 1 cm s^{-1} and E_c, the collection efficiency of cloud droplets for carbon black dust is 10^{-4}. A comparison of (5) and (6) shows that the diffusion effect is about two-orders-of-magnitude larger than the swept-out effect.

3) SINK DUE TO RAINDROPS

(i) Diffusion effect. Carbon black particles diffuse onto the surface of raindrops. Similar to (5), this sink term is

$$\frac{\Delta C_b}{\Delta t} = -4\pi D_b C_b\int_0^\infty\left(\frac{D_R}{2}\right)N_{0R}\exp(-\lambda_R D_R)dD_R = \frac{-2\pi D_b C_b N_{0R}}{\lambda_R^2}. \quad (7)$$

(ii) Sweep-out effect. Raindrops collect carbon black particles. Similar to (6), this term is

$$\frac{\Delta C_b}{\Delta t} = -\pi a C_b E_R\int_0^\infty\left(\frac{D_R}{2}\right)^2 D_R^b N_{0R}\exp(-\lambda_R D_R)dD_R = \frac{-\pi a C_b E_R N_{0R}\Gamma(3+b)}{4\lambda_R^{3+b}}, \quad (8)$$

where E_R, the collection efficiency of raindrop for carbon black dust, is 0.5×10^{-4}, $a=2115$ cm^{1-b} s^{-1} and $b=0.8$. Comparison of (7) and (8) shows that the sweep-out effect is about three orders of magnitude larger than the diffusion effect.

These sink terms are our first attempts at approximating the depletion of carbon dust in the clouds. Possibly

other processes are operating, such as diffusiophoresis or electrical effects, which would tend to increase the loss within clouds and rain, or aggregation in clear air. Agglomeration is a very complex process and has yet to be sorted out completely.

d. Thermodynamic energy equation

We modify the thermodynamic energy equation in Orville *et al.* (1972) to obtain

$$\frac{\partial \phi'}{\partial t} = -\mathbf{V}\cdot\nabla\phi' + \nabla\cdot K_h \nabla\phi' - \frac{\partial T}{\partial z}\left[\frac{C_w}{C_p T_{00}} l_{cw} w + (w - V_t) l_R \frac{C_w}{C_p T_{00}}\right] - \frac{\partial T}{\partial x}\left[u\left(\frac{C_w}{C_p T_{00}} l_{cw} + l_R \frac{C_w}{C_p T_{00}}\right)\right] + \frac{\Delta h}{C_p T_{00} \rho \Delta z}, \quad (9)$$

where Δh is the net heat absorbed by carbon black dust (Table 1). In (9), ϕ' is related to entropy, $\mathbf{V}$ is velocity with components u (horizontal) and w (vertical), K_h a nonlinear eddy coefficient for heat, T temperature, C_w and C_p specific heats for water and air at constant pressure, respectively, and T_{00} a reference temperature. In (9), the effect of carbon black dust is the last term. The procedure for calculating the temperature is the same as in Orville *et al.* (1972).

e. Computation scheme

The computation of advection for all fields except carbon black dust uses Crowley's second-order advective differencing technique (Crowley, 1968). A time step of 15 s is used initially and is reduced to maintain numerical stability as the wind speed increases.

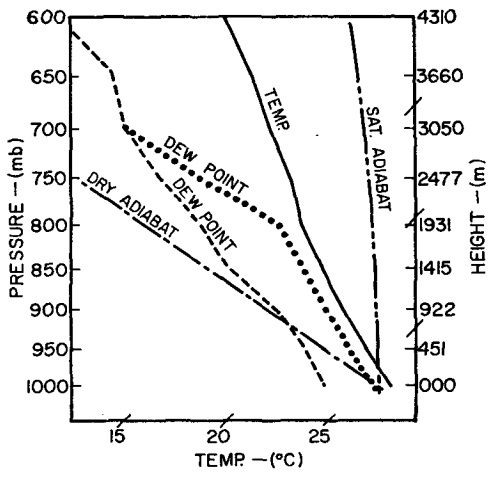

FIG. 1. Portions of the skew-T log P chart showing the initial thermodynamic conditions for the Even, Layer-A and Layer-B cases. Solid dots are used for the Layer-B case; the dashed curve is for the other two cases.

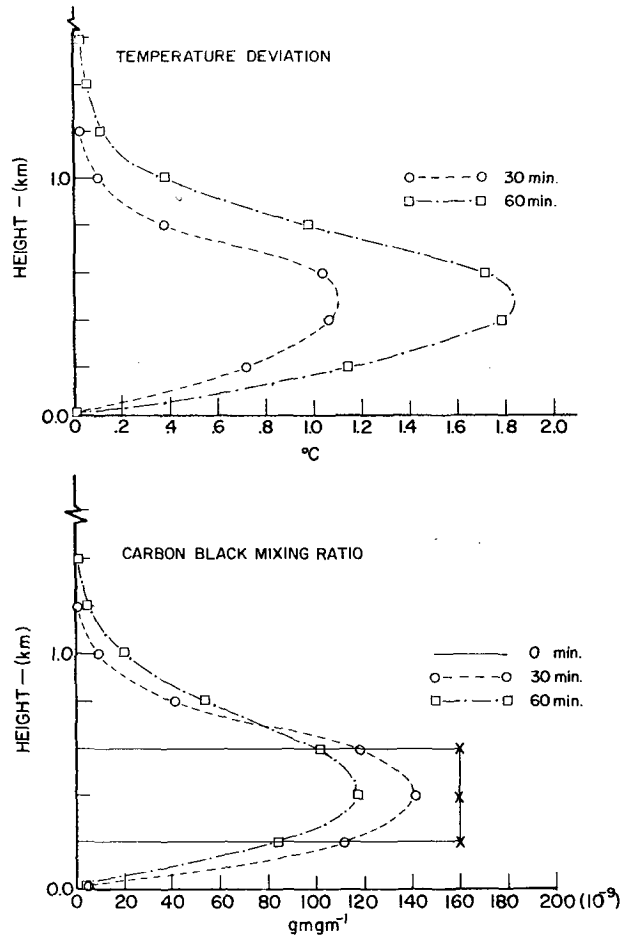

FIG. 2. The initial distribution of carbon black for the Even case and results for the distribution of carbon black and temperature difference from the initial value at 30 and 60 min for the Even case.

The advection technique for carbon black dust is adapted from a method developed by Rainer Bleck for advecting hydrometeors in an axisymmetric cloud model (unpublished manuscript, NCAR). We consider a grid point with $C_b \gtrless 0$ and assign an air volume to it which is a cubical volume centered at this point. Carbon black dust is assumed to fill this volume uniformly and then the volume is moved in x and z directions by the proper amount $\mathbf{V}\Delta t$. In this process, it will occupy space originally assigned in the same manner to the surrounding grid points, thereby moving a well-determined quantity of carbon black dust into those neighboring volumes. Details of the scheme are given in a thesis by Chen (1975).

The advantages of this scheme are that the mass of carbon black dust is conserved and no negative values appear; but being a first-order scheme, numerical diffusion of carbon black dust occurs.

Forward time differences and centered differences in space are used in this model except for the wind speed calculation at the upper and lower boundaries' grid

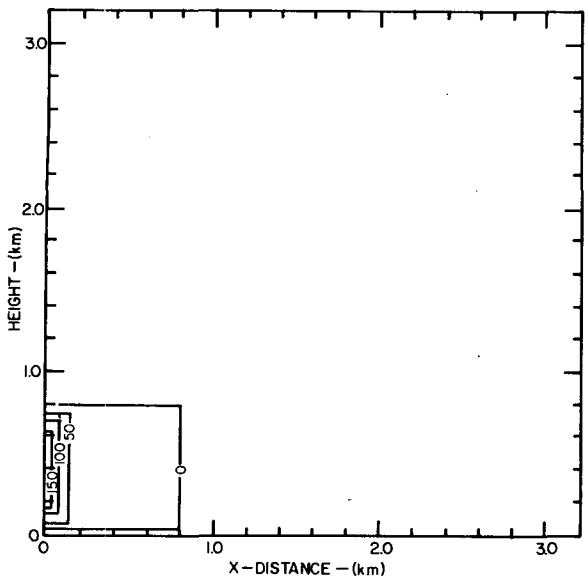

FIG. 3. The initial distribution of carbon black for the Layer-A and Layer-B cases. The contour interval is 50×10^{-9} g g^{-1}.

points. Non-centered finite differencing is applied when the wind at the boundaries is calculated from the stream-function. The wind field is computed from the stream-function which is computed by solving Poisson's equation using a direct method (Buneman, 1969; Buzbee *et al.*, 1970; Rognlie and Kopp, 1976).

The grid space Δx in the horizontal direction and Δz in the vertical direction are set at 200 m; a Δz of 10 m is applied in the lower boundary layer.

f. Boundary conditions

The lower boundary of the model is set at 10 m above the ocean surface. The water vapor at the lower grid points is assumed to remain constant at its initial value.

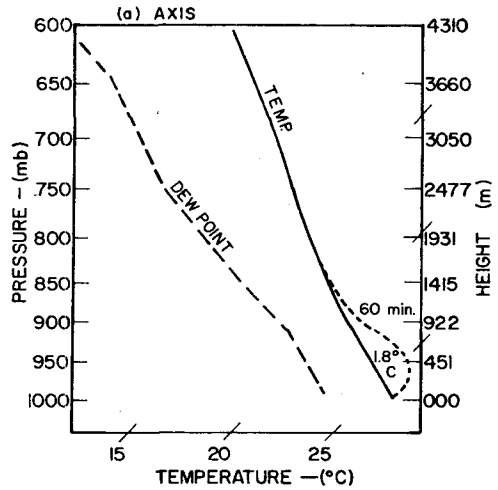

FIG. 4. The thermodynamic conditions for the Even case. Original curves are at the initial time and changes are shown for 60 min.

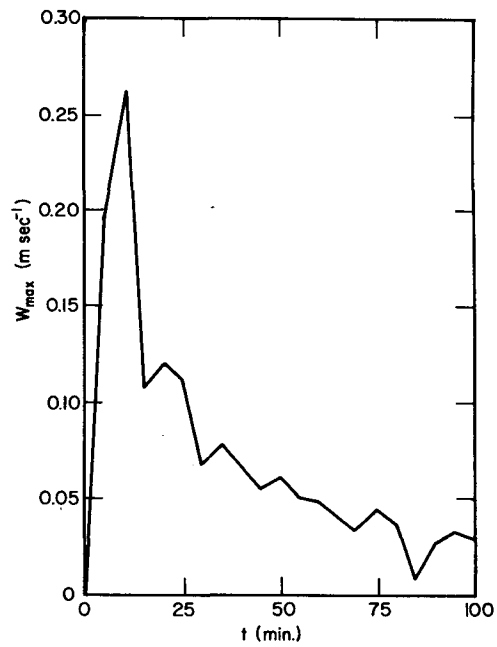

FIG. 5. Time variation of W_{max} at the axis for the Layer-A case.

Only tangential flow exists at any boundary. The stream function and vorticity vanish at all boundary grid points. It is hoped that the lateral boundaries are far enough from the weak disturbances to have little effect on the solution. Other experiments on other physical situations (Orville, 1968) have shown negligible effects if the disturbance is relatively far from the side boundaries.

g. Initial conditions

Initially the atmosphere is assumed stratified and stable. Three cases are considered in this numerical study. These are labeled Even, Layer-A and Layer-B. The initial thermodynamic conditions for the Even and Layer-A cases are based on the statistics of Jordan (1958). Recent work by Gray *et al.* (1976) indicates a more humid sounding could be used in future work. Fig. 1 shows the initial thermodynamic conditions used in these cases. Modification of the dew-point curve of Fig. 1 gives the initial thermodynamic conditions for the Layer-B case. This change is made to allow the formation of cloud more easily so that we can study the effect of clouds on carbon black dust.

Fig. 2 gives the initial distribution of carbon black for the Even distribution case. The initial distribution of carbon black for Layer-A and Layer-B cases is presented in Fig. 3. The average percent area coverage is about 10% in every case but the Even case, which is 36% (not a realistic situation).

A minimum eddy diffusivity, 10 m^2/s^{-1}, for heat, vapor and carbon black transfer in the atmosphere is assumed in the computation of K_m and K_h and is, in

fact, the value most often used because of the weak motions in the cases run.

4. Results and discussion

a. Even case

The initial distribution of carbon black dust in this case and the general results are shown in Fig. 3. Because there are no horizontal gradients of carbon black dust, no horizontal temperature gradients develop. An examination of the vorticity equation shows that no organized air motion will be generated in this case. Therefore, the only way to redistribute carbon black dust is by diffusion. Initially, carbon black dust is horizontally homogeneous and remains so for all time, as indicated in Fig. 2 for 30 and 60 min. Carbon black particles diffuse upward and down to the ocean. Also Fig. 2 displays the temperature difference from the initial temperature value at 30 and 60 min. Solar energy heats the air only where carbon black dust exists. Fig. 4 shows that there is an obvious change in temperature at 60 min modifying the sounding significantly. No significant change in dew point occurs because there is no organized air motion. A slight change in dew point (the maximum change corresponds to a change of 0.2 g kg^{-1} in water vapor mixing ratio) is due to the diffusion effect (but not shown in the figures).

This case shows that the heating rates in the thermodynamic equation source term are correct and that the model is operating correctly with respect to the carbon dust heating; no motions are generated. These results indicate that carbon black spread over large regions will not disperse rapidly if horizontal gradients of the carbon black are minimal (zero). However, the results also indicate a scale limitation to the model. In the atmosphere, such heating would lead to falling pressures over an extensive area and the initiation of mesoscale motions with upward motion in the heated region, downward on the periphery. These concepts can be checked in larger, more extensive domain models, both cloud-scale and meoscale.

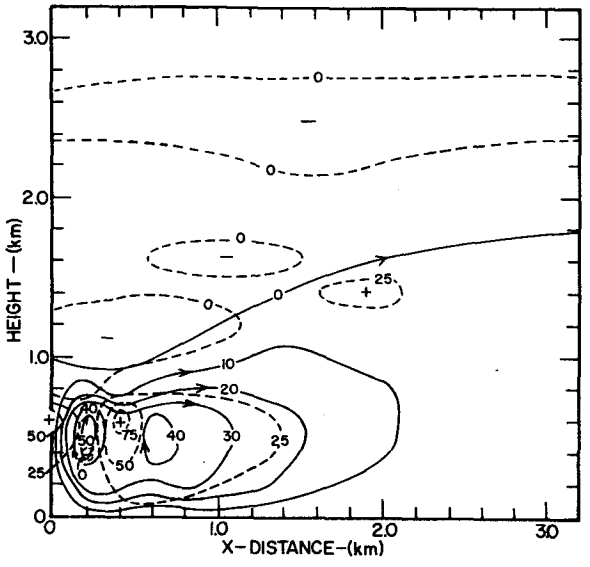

FIG. 6. The streamfunction (solid lines) for the Layer-A case at 10 min, contour interval 10 kg m^{-1} s^{-1}, and the virtual temperature difference (dashed line) from the initial state at 10 min for the Layer-A case, contour interval 25×10^{-3}°C.

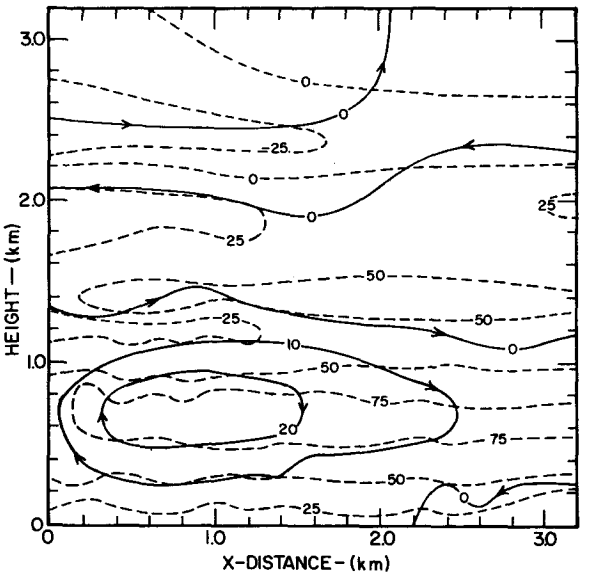

FIG. 7. As in Fig. 6 except at 50 min.

b. Layer-A case

The initial distribution of carbon black dust in this case is shown in Fig. 3. The horizontal gradations of the carbon black concentration produce gradients in the heating rate which lead to the development of horizontal

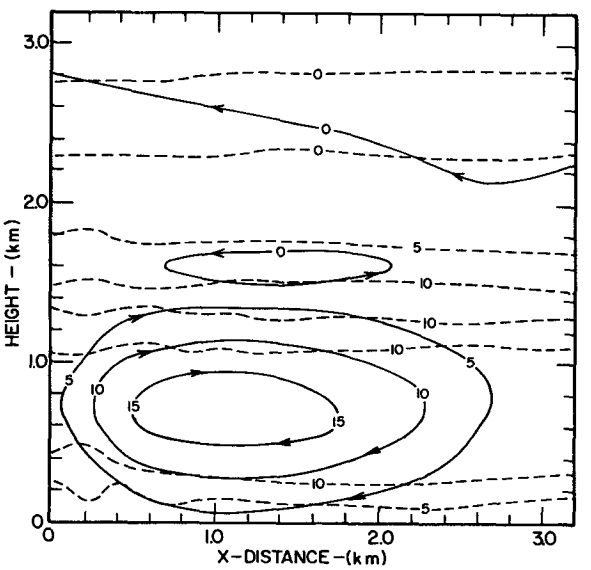

FIG. 8. As in Fig. 6 except at 100 min. The contour intervals are 5 kg m^{-1} sec^{-1} (streamfunction) and 5×10^{-2}°C (temperature difference).

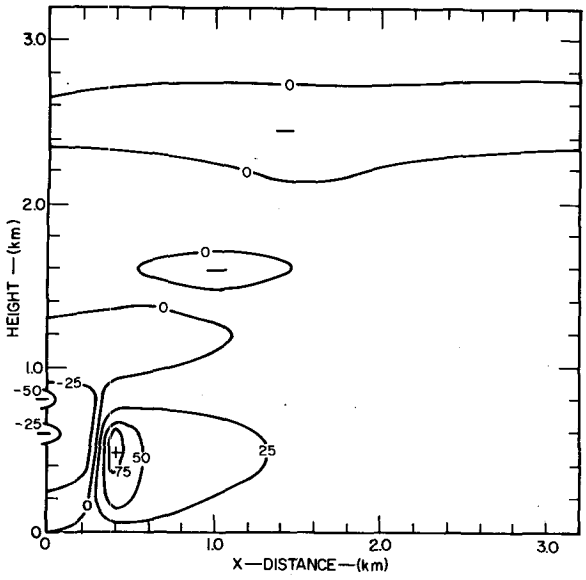

FIG. 9. The temperature difference from the initial value at 10 min for the Layer-A case. The contour interval is 25×10^{-3}°C.

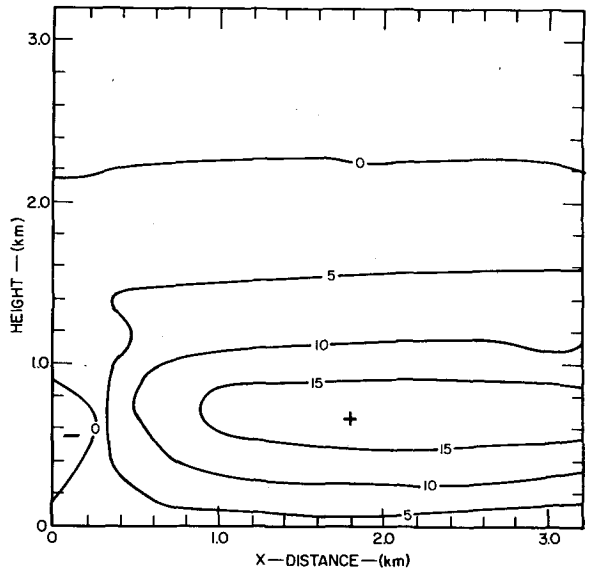

FIG. 11. As in Fig. 9 except at 100 min. The contour interval is 5×10^{-2}°C.

temperature gradients and resulting circulation. Fig. 5 shows the time variation of the maximum vertical velocity W_{max} at the axis. At 10 min, W_{max} reaches its maximum value, 0.27 m s^{-1}, then decreases very rapidly as time increases. An oscillation due to the stable atmosphere appears. Also, the streamfunction shows that the flow is strong in the first 10 min and then becomes weaker (Figs. 6–8). The reason for this phenomenon is that the heating source has strong horizontal gradients in the first 10 min. After that, the heating source is redistributed and the gradients weaken. The sensible temperature at the axis is lower than that in the environment because the advective cooling works against carbon black heating (Figs. 9–11). However, the virtual temperature in the lower atmosphere is higher at the axis in the first few tens of minutes (Figs. 6–8). The buoyancy of an element is proportional to the virtual temperature difference between the element and the environment; hence, the circulation is stimulated initially but weakens noticeably at later times. These results show the net effect of the heating due to carbon black and the cooling due to updraft.

Fig. 12 shows the time variation of total amount of carbon black. (Multiplication by $\Delta x\,\Delta y\,\Delta z = 9\times10^{12}$ cm^3 yields about 5.6 kg of carbon black dust total.) This curve decreases with time except in the first 2.5 min. This slight increase (0.27% of the original value) is due to the noncentral numerical technique for the vertical ∇^2 term in the diffusion effect at the lower boundary. After 100 min, the total mass of carbon particles is

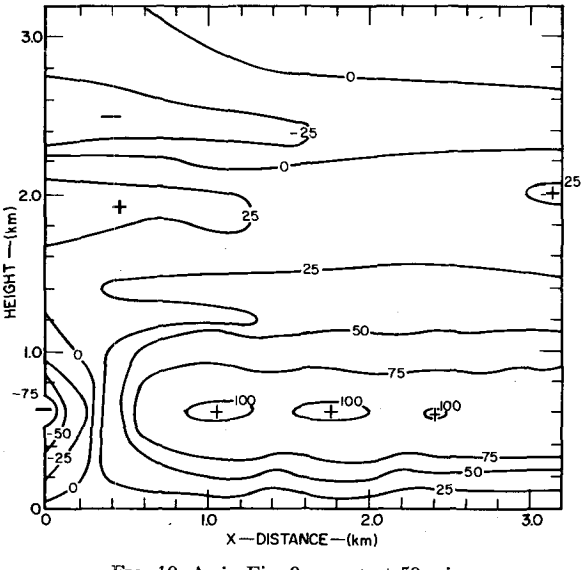

FIG. 10. As in Fig. 9 except at 50 min.

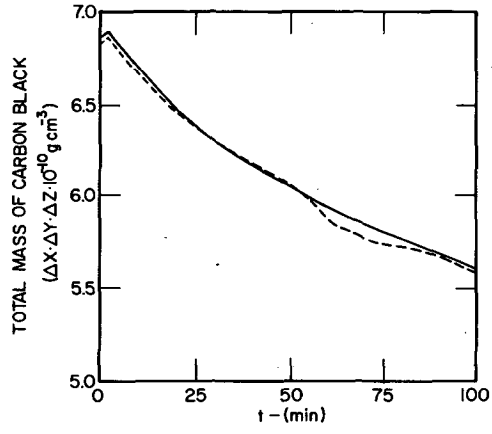

FIG. 12. Time variation of the total mass of carbon black remaining in the cloud model domain for the Layer-A case (solid) and the Layer-B case (dashed).

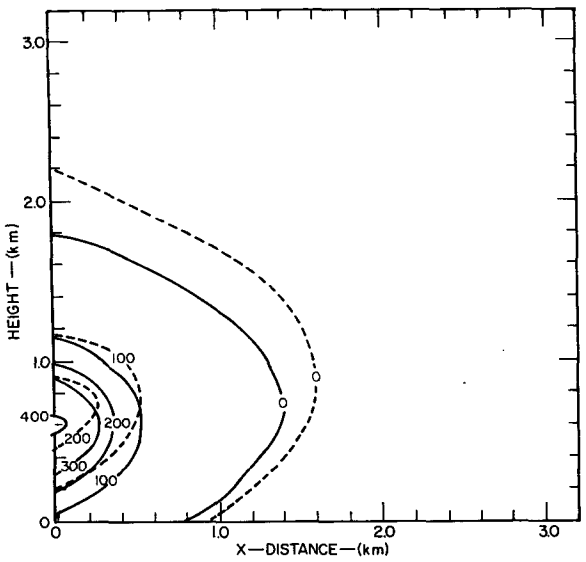

FIG. 13. The distribution of carbon black at 50 min (solid) and 100 min (dashed) for the Layer-A case. The contour interval is 100×10^{-10} g g^{-1}.

about 82% of the original value. The only way to lose carbon black in this case is by diffusion to the ocean surface. In the first 25 min, the rate of loss for carbon black is larger than at later times. This phenomenon can be understood by analyzi ıg the vertical gradient of carbon black concentration near the lower boundary. Initially, it is large. After 25 min, this large gradient becomes weaker because of advection and diffusion of the carbon black. Consequently, the rate of loss of carbon black decreases. Fig. 13 gives evidence that the distribution of carbon black is smoothed out by the advection and diffusion effects.

Fig. 14 shows that no cloud will form in this case because of the large difference in the dew-point and and temperature curves. The dew-point curve is modified very prominently (maximum change corresponds to 0.9 g kg^{-1}) at the axis, although the temperature curve has no obvious change. The temperature curve at a column 3 km away from the axis shows a slight rise after 100 min because of subsidence. Slight drying occurs (mixing ratio decreases by 0.2 g kg^{-1}), but it is too small to be shown in Fig. 14. The primary result of this case is the initial small, sensible heating causing sensible temperature excesses followed later by actual sensible temperature deficits (cause by an imbalance between radiational heating and adiabatic cooling in the updraft). The increase of moisture along the axis leads to a slight virtual temperature excess which maintains the motion.

This case shows that atmospheric circulations are generated by the horizontal gradients of carbon black. Relatively strong motion occurs in the first 10 min and then becomes weak very quickly. Oscillations due to the stable atmosphere also appear. Cooling and moistening in updrafts as well as warming and drying in downdrafts are the effects of the air motion. Also, very importantly, these results demonstrate *the tendency of small-scale atmosphere convection to smooth out temperature differences but to create strong humidity differences.*

Another test of interest would be a fairly even distribution of carbon black superimposed on random perturbations of temperature and water vapor. This would probably lead to a more rapid dissipation and spread of the carbon black because the magnitude of the motions produced by such perturbations is greater than that produced by the carbon dust (Hill, 1974; Chang and Orville, 1973).

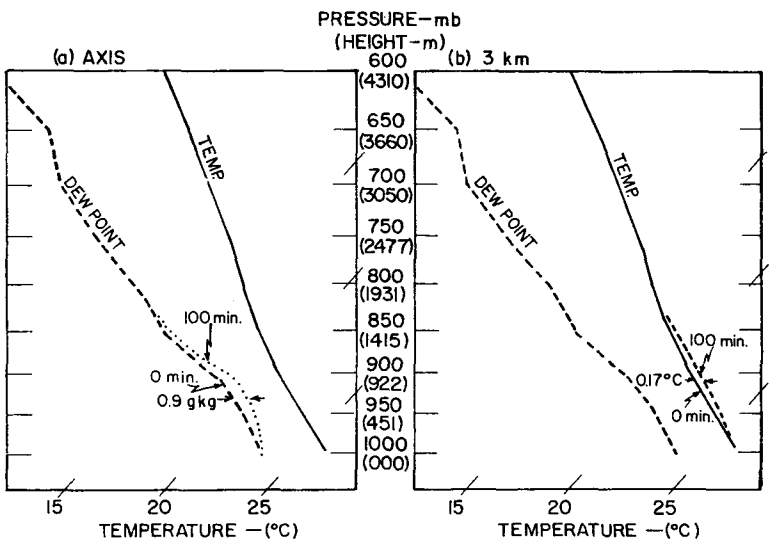

FIG. 14. The thermodynamic conditions for the Layer-A case for the axis (a) and for a column 3 km away from the axis (b). Original curves are at the initial time, and changes are shown for 100 min.

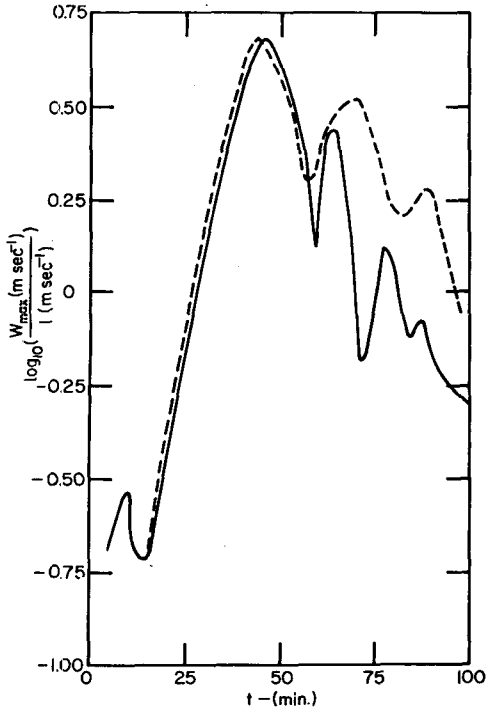

FIG. 15. Time variation of W_{max} for the Layer-B case with cloud and rain albedo (solid) and without cloud and rain albedo (dashed).

c. Layer-B case

The initial thermodynamic conditions for this case are shown in Fig. 1. The atmosphere is arbitrarily enriched with moisture to encourage cloud formation. The same initial distribution of carbon black as in the Layer-A case exists (Fig. 2). A cloud forms at 12.25 min and dissipates at 95.25 min.

Fig. 15 presents the curves of W_{max} on the axis versus time with a log transformation used along the ordinate. After cloud formation, this velocity increases with time until it reaches a maximum value of 4.6 m s^{-1} at 48.25 min. After the cloud passes its mature stage, W_{max} decreases with time but has some oscillation. Figs. 16 and 17 show the distribution of cloud water and rainwater at 48.25 and 60.25 min, respectively. At 60.25 min, this cloud produces its maximum intensity of rain, of order 10^{-2} g kg^{-1}. Figs. 16 and 17 show that a small cloud forms. Fig. 18 displays the distribution of carbon black at 48.25 and 95.25 min. In these figures, we see that a "tongue" of carbon black is generated by the advection effect. Because stronger air motion occurs in this case, the carbon black particles fill almost the whole domain but without any strong gradients at 95.25 min.

Fig. 19 shows that the total amount of carbon black removed by the cloud water and rainwater is 2.27×10^{-12} $\Delta x\Delta y\Delta z$ [g cm^{-3}], which is 0.33% of the original carbon black. Since the radius of carbon black particles is 1% of that of the cloud water droplets, it is difficult for the

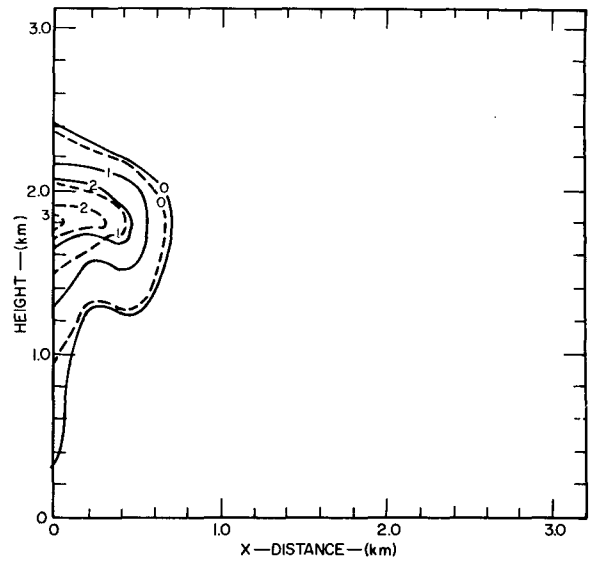

FIG. 16. The distribution of cloud water (solid) and rain water (dashed) at 48.25 min for the Layer-B case. The contour interval is 1.0 g kg^{-1} for cloud water and 10^{-2} g kg^{-1} for rain water.

cloud water and raindrops to collect the carbon particles. Besides, these results are for a small cloud so that cloud effects on carbon black are not very evident. The total carbon black remaining in the cloud model at 100 min is 81.8% of the initial value (Fig. 12). In the first 25 min, the slope of this curve is steeper because stronger vertical gradients of carbon black concentration exist near the lower boundary of the cloud model. After that, the slope of total carbon black versus time curve decreases until 48 min when the slope increases slightly. During the 48–60 min period, the quantity of cloud water and rainwater is higher. After the cloud

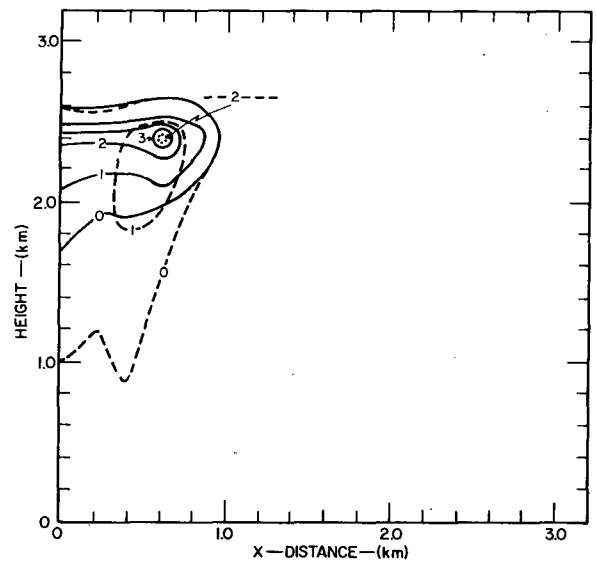

FIG. 17. As in Fig. 16 except at 60.25 min. The contour interval is 10^{-1} g kg^{-1} for rain water.

dissipates, the total amount of carbon black decreases very slowly by diffusing down to the ocean surface. Comparison of the total amount of carbon black remaining in the atmosphere at 100 min in the Layer-A and Layer-B cases shows nearly equal quantities. The slight difference is due to the cloud and rain effects.

When the cloud and rain albedo effects are eliminated, W_{max} is affected (Fig. 15); it reaches its maximum value 3 min earlier than in the situation when the cloud and rain albedo are considered. Turning off these effects leads to a W_{max} value 15 cm s^{-1} higher. Before 55 min, the difference between the two curves in Fig. 15 is minimal. After 55 min, the difference is large because of the effect of the reduction in insolation due to the cloud and rain. Maximum cloud development occurs at about 50 min, although maximum cloud water content occurs at about 60 min. These cloud effects on carbon black are small, but only a small cloud has been simulated. Little carbon black dust (less than 1% of the initial carbon black) is scavenged by the cloud and rain particles. The cloud effects on the vertical velocity are much more evident. The vertical velocity would be larger if the small amounts of cloud and rain did not reduce the solar energy absorbed by carbon black dust.

Two other cases were run but are not shown here. A "bubble" case was run to test the effects of a different distribution of carbon black dust. Results were similar to the Layer-A case. Changing the temperature curve in the mean sounding to simulate an inversion layer while using the same initial carbon dust distribution as in the Layer-A case resulted in an "Inversion" case. This case showed that an inversion layer would limit air motion and restrict the dispersion of carbon black dust.

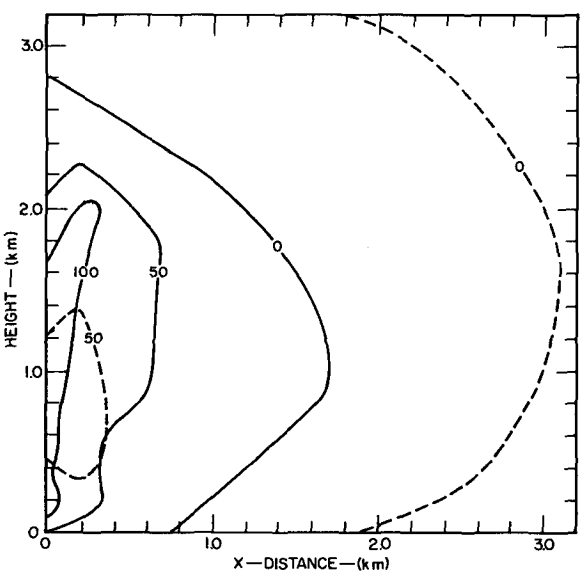

FIG. 18. The distribution of carbon black at 48.25 min (solid) and at 95.25 min (dashed) for the Layer-B case. The contour interval is 50×10^{-10} g g^{-1}.

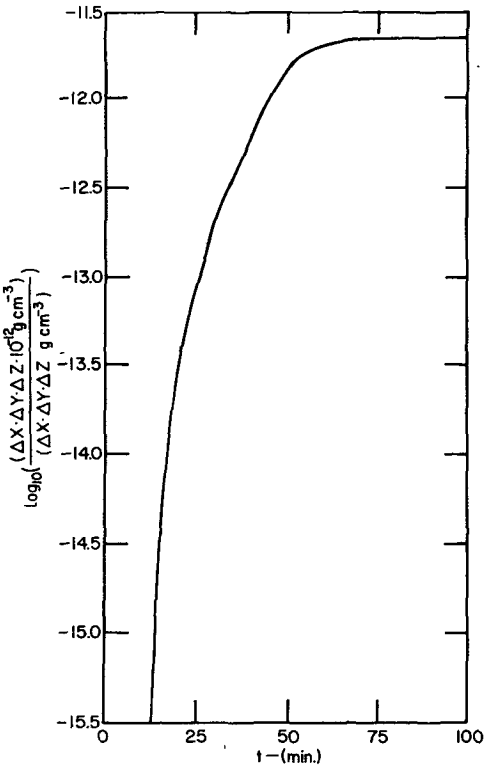

FIG. 19. Time variation of the cumulative carbon black collected by cloud water and rain.

5. Concluding remarks

Carbon black dust can absorb solar energy and then transfer almost all of the absorbed energy to the surrounding air. A 10% area coverage can produce a vertical velocity of ~30 cm s^{-1} in 10 min on the cloud scale. However, the vertical velocity decreases with time very rapidly because the heating rate is proportional to the concentration of carbon black which is redistributed by diffusion and avection effects. Horizontal gradients have to be minimized to keep spreading and dilution at a minimum. Two hours later, the vertical velocity is about 2 cm s^{-1}. This 2 h duration is quite small compared to the 1–2 day duration suggested by Gray *et al.* (1976), which emphasizes the difference in this simulation and the broad-scale effects hypothesized by Gray.

Water vapor is pumped up in the updrafts. Net cooling occurs along the axis in the updrafts, which are driven by positive virtual temperature differences. Subsidence warming and drying occur in the downdrafts. Sensible temperature differences are smoothed out, while humidity differences are strengthened by the convection. Of the initial carbon black 82–85% remains in the cloud model domain after 100 min, the loss being accounted for by diffusion to the ocean surface. Increasing the average area coverage would cause stronger motion, but the decrease of vertical velocity with time would still happen. A small cloud has almost no effect on the total amount of carbon black dust, but does cut

off some of the solar insolation to the carbon dust, reducing the heating effect and the associated circulation.

These results do not support the previous cumulus generation hypothesis of Van Straten *et al.* (1958) on carbon dust enhanced individual cloud formation. We used larger amounts of carbon black dust in the simulations than in the field experiments and had to artificially moisten the atmosphere to obtain small cloud formation. However, no direct comparison was made with a sounding taken from the field operations.

Our results are not directly applicable to the Gray *et al.* (1976) hypothesis on mesoscale weather modification by carbon dust seeding. They do, however, indicate that the cumulus response for a particular sounding of the tropical lower atmosphere for boundary layer carbon dust heating is less than what might be generally expected. This should allow for more solar energy accumulation than would occur if a rapid cumulus response to the solar heating were to result. The chances for larger space and time scale convective alterations are better if the carbon particles are not rapidly lost to cloud agglomeration or surface capture, or if attenuation of solar energy gain by upper layered clouds does not occur.

Further studies in larger domain cloud models and in mesoscale models are needed to see if cloud formation would occur as a result of a broader distribution of carbon black and a longer exposure to solar heating which would influence mesoscale circulations.

Acknowledgments. We wish to express our sincere thanks to Drs. Philip C. S. Chen and C. S. Chiu for their helpful suggestions. Appreciation is extended to Mr. Fred Kopp for his discussions and aid in running the program.

We thank Dr. William Gray for stimulating our interests in this topic.

This research was supported by the National Science Foundation under Grant ATM75-03882.

REFERENCES

Buneman, O., 1969: A compact non-iterative Poisson solver. Rep. SUIPR-294, Institute of Plasma Research, Stanford University, 11 pp.

Buzbee, B. L., G. H. Golub and W. Nielson, 1970: On direct methods for solving Poisson's equation. *SIAM J.*, **7**, 627–656.

Byers, H. R., 1965: *Elements of Cloud Physics*, 2nd ed. The University of Chicago Press, 191 pp.

Chang, W. J., and H. D. Orville, 1973: Large scale convergence in a numerical cloud model. *J. Atmos. Sci.*, **30**, 947–950.

Chen, C. S., 1975: The effects of carbon black dust on convection. M.S. thesis, Dept. of Meteorology, South Dakota School of Mines and Technology, Rapid City, 75 pp.

Crowley, W. P., 1968: Numerical advection experiments. *Mon. Wea. Rev.*, **96**, 1–11.

Downie, C. S., 1960: Cloud modification with carbon black. *Cumulus Dynamics*, C. E. Anderson, Ed., Pergamon Press, 191–208.

Drake, R. L., P. D. Coyle and D. P. Anderson, 1974: The effects of nonlinear eddy coefficients on rising line thermals. *J. Atmos. Sci.*, **31**, 2046–2057.

Frank, W. M., 1973: Characteristics of carbon black dust as a large-scale tropospheric heat source. Res. Rep. No. 195, Dept. of Atmospheric Science, Colorado State University, 52 pp.

Fuchs, N. A., 1964: *The Mechanics of Aerosols*. MacMillan, 408 pp.

Gray, W. M., W. M. Frank, M. L. Corrin and C. A. Stokes, 1974: Weather modification by carbon dust absorption of solar energy. Res. Rep. No. 225, Dept. of Atmospheric Science, Colorado State University, 191 pp.

——, ——, —— and ——, 1976: Weather modification by carbon dust absorption of solar energy. *J. Appl. Meteor.*, **15**, 355–386.

Hill, Geoffrey E., 1974: Factors controlling the size and spacing of cumulus clouds as revealed by numerical experiments. *J. Atmos. Sci.*, **31**, 646–673.

Jordan, C. L., 1958: Mean soundings for the West Indies area. *J. Meteor.*, **15**, 91–97.

Liu, J. Y., and H. D. Orville, 1969: Numerical modeling of precipitation and cloud shadow effects on mountain-induced cumuli. *J. Atmos. Sci.*, **26**, 1283–1298.

Orville, H. D., 1968: Ambient wind effects on the initiation of cumulus clouds over mountains. *J. Atmos. Sci.*, **25**, 385–403.

——, W. J. Chang and F. J. Kopp, 1972: A numerical experiment on the simulation and modification of hurricane rainband clouds; final report. Rep. 72-12, Inst. Atmos. Sci., South Dakota School of Mines and Technology, Rapid City, 80 pp.

Paltridge, G. W., 1974: Infrared emissivity, short-wave albedo, and the microphysics of stratiform water clouds. *J. Geophy. Res.*, **79**, 4053–4058.

Rognlie, Dale M., and Fred J. Kopp, 1976: Application of direct Poisson solvers to time-dependent numerical cloud models. *Mon. Wea. Rev.*, **104**, 7, 953–960.

Van Straten, F. W., R. E. Ruskin, J. E. Dinger and H. J. Mastenbrook, 1958: Preliminary experiments using carbon black for cloud modification and formation. Rep. No. 5253, U. S. Naval Research Laboratory, 17 pp.